Near edge tractions for a rounded quarter-plane pressed into an elastically similar half-plane

B. Eames *, D.A. Hills, M.R. Moore

Department of Engineering Science, University of Oxford, Parks Road, Oxford, OX1 3PJ, UK

ARTICLE INFO

ABSTRACT

Asymptotic forms are a useful way of representing the state of stress at a contact edge, allowing us to characterise the region in which cracks nucleate. The asymptotes must match the behaviour implied by the local geometry. In this paper, we study the behaviour of a flat contact with a circular arced edge (i.e. a flat and rounded contact); a geometry that has extensive applications. We show explicitly how the very convenient closed-form solution for this problem, derived from half-plane theory, may be collocated into the more realistic three-quarter plane far field solution, obtained from Williams' solution. This provides a closed-form representation of the edge, correctly geared to the far-field solution, for the first time.

1. Introduction

Our high-level goal is to produce a rigorous match between prototypical problems suffering from fretting fatigue and the conditions present in laboratory experiments measuring fretting strength, with the intention of applying the idea to a wide range of applications. Cracks invariably start at or very near the contact edge [1]. The general philosophy is to match by using a set of asymptotic forms to describe the hinterland, a method which we have developed here over several years [2–4], and which has also been independently developed [5–7], in a slightly different form. We restrict ourselves to problems in which the contact is convex in form, and hence incomplete in character. This means that very close to the edge of the contact, and regardless of whether or not the contact overall may be described using half-plane theory, local surface tractions and corresponding displacements will be related by Flamant (half-plane) theory. Hence the contact pressure, $p(x)$, and shear traction, $q(x)$ may always be approximated by a single term, square root bounded in form, defined by a multiplier, L_I and L_{II} respectively so that

$$p(x) = L_I \sqrt{x} + O(x^{3/2}) \quad \text{as} \quad x \to 0, \tag{1}$$

$$q(x) = L_{II} \sqrt{x} + O(x^{3/2}) \quad \text{as} \quad x \to 0, \tag{2}$$

where x measures distance from the left-hand contact edge, as depicted schematically in Fig. 1. In practice, this single term may only apply over a very small distance from the contact edge and it is the goal of this paper to both categorise this and offer a possible remedy.

Later in this paper, we will investigate the different formulations of the problem for both pure mode I and II loading, as in [8]. Mode I loading is when the stress is orthogonal, and mode II when the stress is parallel, to the bisector of the three-quarter plane. Fig. 1 is a schematic representation of the incomplete contact between a semi-infinite flat and rounded punch (Body 1) and a half-plane (Body 2). $K_{I[1/2]}$ and $K_{II[1/2]}$, displayed in Fig. 1, are the square-root singular multipliers on modes I and II loading which emerge from the half-plane formulation. For an observation point remote from the contact edge, the edge radius becomes insignificant, and, if there is no remote slip, the domain can resemble a three-quarter plane (i.e. a large wedge of angle $3\pi/2$). $K_{I[3/4]}$ and $K_{II[3/4]}$, also labelled in Fig. 1, are the generalised stress intensity factors, acting as multipliers on Williams' modes I and II eigensolutions, in a wedge sense (cf. [9,10] for an extensive discussion of the Williams' solution).

Irreversibilities occur in the 'process zone'. The approach outlined hinges on the process zone being contained wholly within a hinterland in which the (L_I, K_{II}) fields dominate the character of the (elastic) state of stress. We have recently looked at the properties of series expansions of the near-edge fields, beyond the first term [11]. Here we will just repeat, briefly the results of a representation of the singular shear traction:

$$q_{\text{local}}(x) = \frac{K_{II}^{\pm}}{\sqrt{x}} + L_{II}^{\pm}\sqrt{x} + M_{II}^{\pm}(x)^{3/2} + O\left(x^{5/2}\right) \quad \text{as} \quad x \to 0, \tag{3}$$

where the multipliers are given in [11] and show that the first term alone captures the state of stress well for a significant fraction of the contact size in a Hertzian contact.

---

* Corresponding author.
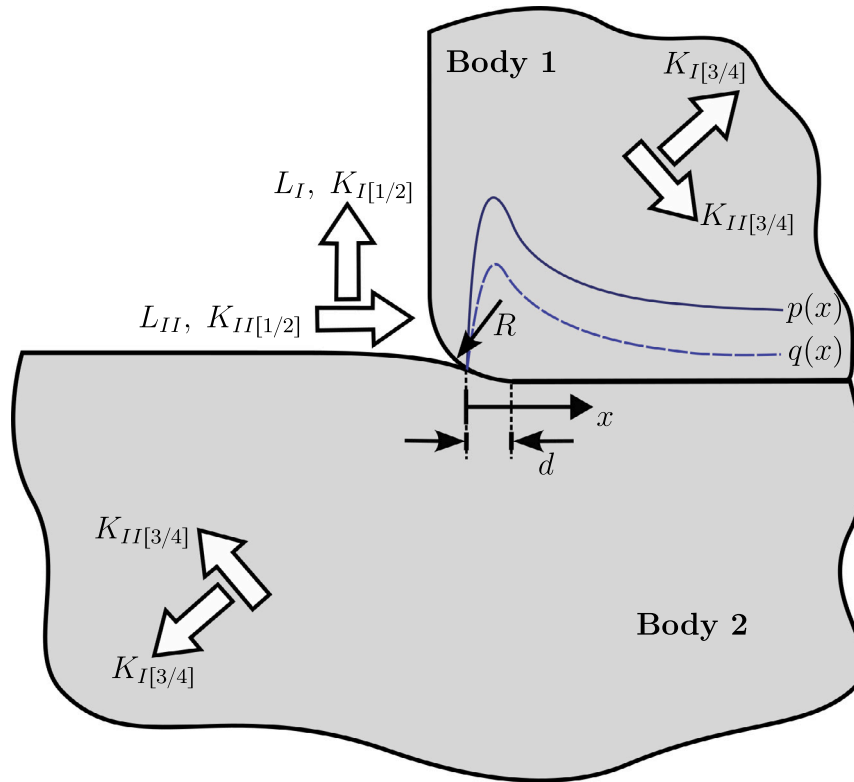 *E-mail address:* beth.eames@eng.ox.ac.uk (B. Eames).

Fig. 1. Here, x denotes distance from the left-hand edge of the contact region, d denotes the length of the curved section in the contact, R the radius of curvature of the rounded part of the punch. $K_{I[3/4]}$, $K_{II[3/4]}$ and $K_{I[1/2]}$, $K_{II[1/2]}$ are the generalised stress intensity factors acting as multipliers for modes I and II, for a three-quarter plane and half-plane formulation, respectively. Illustrative profiles of the contact pressure $p(x)$ and shear tractions $q(x)$ are indicated for reference.

Many of the early tests on fretting fatigue strength, when our under-standing of its mechanics was in its infancy, used the Hertzian contact. However, a great many practical contacts have a central flat form, say of half-length b, and end radii, R, such as the finite punch displayed schematically in Fig. 2(a). Applications include contacts found in the root of gas turbine fan blade dovetails [12], or in the locking segments of riser-seabed connectors. Analysing these problems introduces several new features. The first is the question of how well the asymptotic expansion near the contact edge models the contact pressure. Assumptions include that, in this region, the contact is well represented by half-plane theory, which is treated in the next section. Secondly, a deeper question then surfaces of how interior properties of the contact, where half-plane theory does not apply, control the overall properties of the contact. In particular, what happens at the contact edge? This aspect is treated comprehensively in subsequent sections.

2. Asymptotic representation of the state of stress

One method to improve the fidelity of the solitary term, Eq. (1), is to employ an asymptotic expansion, including higher-order terms in the asymptotic approximation. Considering d, the contact length in the curved section, and $2b$, the flat length of the contact, permits us to have solutions for three different types of contacts:

- Hertzian contacts, $b/d \to 0$;
- finite contacts, b/d is finite;
- semi-infinite contacts, $b/d \to \infty$.

We discuss these in turn.

2.1. Hertz ($b/d \to 0$)

The exact solution for the normal contact pressure in the Hertz case [10] can be written as

$$p(x) = -\frac{2P\sqrt{d^2 - (x-d)^2}}{\pi d^2}, \tag{4}$$

where P is the constant downward normal force from the contact (see, for example, [10]). For the Hertz problem, we note that the entire contact length is curved: thus, d is also considered the half-length of the entire contact.

As seen in [13], the multiplier L_I may be shown to be

$$L_I = \frac{E^*}{R}\sqrt{\frac{d}{2}}, \tag{5}$$

where E^* is the plane strain modulus. In general, the normal force may be related to the contact half-width d via

$$-P(d) = \frac{\pi E^* d^2}{4R}. \tag{6}$$

As the normal force is uniform in the present analysis, i.e. $P(d) = P$, we can rewrite (4) to be in terms of L_I,

$$p(x) = \frac{L_I \sqrt{d}}{\sqrt{2}}\sqrt{1 - \left(\frac{x-d}{d}\right)^2}. \tag{7}$$

Hence, to find the asymptotic form of (7), we can assume x/d is small and take the Taylor expansion for $x/d \ll 1$,

$$p(x) = L_I \sqrt{x}\left(1 - \frac{x}{4d} - \frac{x^2}{32d^2} + O(x^3)\right), \tag{8}$$

so we readily obtain the next two terms in the approximation (as discussed previously in [11]).

2.2. Finite (b/d finite)

For the finite contact case, the exact solution is non-trivial and requires solving an integral equation, which can be found in [11] (see Eq. (20) therein). The expressions for the coefficients of the first three terms in the asymptotic expansion may also be found in [11] as Eqs. (4) and (21)–(23), respectively. We note here that, in [11], 'x' is defined as the coordinate measured from the centre of the contact, rather than the left contact edge. In this paper, we will continue to define 'x' as the coordinate measured from the left contact edge for consistency with the semi-infinite case.

2.3. Semi-infinite (b/d → ∞)

Finally, for the semi-infinite case, when a normal load is applied, the exact solution for the contact pressure induced is given in [14]

$$p(x) = \frac{L_I}{4\sqrt{d}} \left[2\sqrt{dx} + (x-d) \ln \left| \frac{1 - \sqrt{x/d}}{1 + \sqrt{x/d}} \right| \right] \qquad x > 0. \tag{9}$$

Taking a Taylor series expansion of the full solution, we can write the asymptotic pressure distribution in the form

$$p(x) = L_I \sqrt{x} \left(1 - \frac{x}{3d} - \frac{x^2}{15d^2} + O(x^3) \right) \quad \text{as} \quad x/d \to 0 \tag{10}$$

Here, the coefficients scale only with L_1 and the contact size of the rounded section of the punch, d.

2.4. Validity of the asymptotic series expansion

In order to investigate the integrity of these asymptotic expansions in the vicinity of the contact edge, we may re-scale x by d and the asymptotic form of the pressure by $L_I \sqrt{d}$ to facilitate straightforward comparisons with the exact solution. We show these comparisons for the first three terms of the asymptotic expansions in Fig. 2.

We are interested in finding an accurate representation of the internal stress state as far as the slip region extends into the geometry. In practice, slip regions in Hertzian contacts will typically extend to just a small fraction of the contact half-width (here, d). On the other hand, in problems incorporating a flat, it is common for the slip region to extend to a significant fraction of the length d (and, in principle, it might extend beyond the curved region). Therefore, for flat and rounded problems, we may require an accurate representation of the internal stress state as far as $x/d = 1$ in from the contact edge.

For the Hertzian contact (Fig. 2, top), even the two-term solution looks like a decent approximation of the exact solution; when $x/d = 1$, the error of the two-term approximation is only 6.7%. Increasing the number of terms to three or more, improves the approximation even further; for the Hertzian contact, when $x/d = 1$, the error of the three-term approximation is only 1.7%

Unfortunately, this behaviour does not translate to the finite (Fig. 2, middle) and semi-infinite (Fig. 2, bottom) contacts. When using three terms, the finite case approximation is slightly more accurate than the semi-infinite case, however, this is marginal: the errors of the three-term approximations at $x/d = 1$ are 17.5% (for a given finite ratio $b/d = 0.515$) and 20.0%, respectively. To consider a solution appropriate, we may look for errors $< 5\%$ throughout the extent of the slip zone. Therefore, even when using three-term solutions, the asymptotic approximations of finite and semi-infinite contacts are not valid as far as $x/d = 1$ in from the contact edge; asymptotic representations of flat and rounded contacts are poor in this region.

These findings encourage us to consider alternative approaches to finding asymptotic approximations of the exact contact pressure and shear tractions that allow for greater scope and flexibility in problems containing geometries with both flat and rounded parts.

3. Semi-infinite flat punches with rounded edges

An alternative method to using an asymptotic expansion, alluded to in the previous section, is to consider an elastic contact between a half-plane and a semi-infinite indenter with a flat front face and rounded edge. This is attractive as it provides a possible vehicle for encapsulating rounded contact edge behaviour within a lifing procedure. We have made two attempts to find a solution to a contacting pair of this form. The first, [15], used a formulation based on uncoupled half-plane theory. The second, [8], employed a finite element analysis based on a three-quarter plane formulation with a rounded corner for the indenter radii. Before looking at these approaches and showing how they may be employed in tandem, some aspects of the half-plane solution and its attributes merit consideration.

3.1. Half-plane formulation

In a half-plane analysis, the surface tractions and surface normal displacement are related by the following integral equation of the second kind, which stems from Flamant's solution,

$$\frac{dg}{dx} = \frac{2}{\pi E^*} \int_{contact} \frac{p(\xi)\,d\xi}{x - \xi} - \beta q(x), \tag{11}$$

where $p(x)$ is the contact pressure, $q(x)$ is the shear traction present, and $g(x)$ is the relative surface profile. In this equation, the composite plane strain modulus, E^*, is given by

$$\frac{1}{E^*} = \frac{1 - v_1^2}{E_1} + \frac{1 - v_2^2}{E_2} \tag{12}$$

where E_i, v_i are, respectively, the Young's modulus and Poisson's ratio of body i, and β, Dundurs' second constant, is given in [13] by

$$\beta = \frac{E^*}{2} \left[\frac{(1 + v_1)(1 - 2v_1)}{E_1} - \frac{(1 + v_2)(1 - 2v_2)}{E_2} \right]. \tag{13}$$

The solution to the contact problem, therefore, depends on the composite modulus. The mix of stiffness between the two bodies is unimportant in the first (integral) term in Eq. (11), but it is relevant in the second term. This second term physically represents the effect of shear traction on the solution.

We have already alluded to the concept of 'coupling', where the presence of shear tractions causes a change in the relative normal displacement of the contacting surfaces, and, consequently, the contact pressure. To derive a solution from half-plane theory, we are implicitly assuming the contact is 'uncoupled'. For this assumption to be valid, we must agree with two important criteria:

(a) both bodies can be appropriately represented by half-plane domain shapes,
(b) and, the second term in the integral Eq. (11) vanishes.

For the flat and rounded geometry, criteria (a) is only satisfied very close to the contact edge. For this analysis, criteria (b) can only be satisfied by setting $\beta = 0$ as we require a moderate coefficient of friction between the contacting bodies to avoid slip, $q(x) \neq 0$.

To conclude the discussion of 'coupling', in this paper we are only interested in the case were both bodies are elastically similar[1] ($E_1 = E_2$, $v_1 = v_2 \implies \beta = 0$); the solution derived from half-plane theory will be valid, but only when the observation point is very close to the

---

[1] For a different area of study, if the contact-defining body was rigid, its shape outside the contact patch would not figure in the solution; the solution would be the same whether the contact-defining body was a half-plane with a small rounded corner step, or a semi-infinite flat and rounded punch. Therefore, for the unique case where body 1 in Fig. 1 is rigid ($v = 0$) and body 2 is incompressible ($v = 0.5$): we could bypass criteria (a), and criteria (b) would be satisfied as $\beta = 0$; the uncoupled half-plane formulation would be valid for the entirety of the contact.
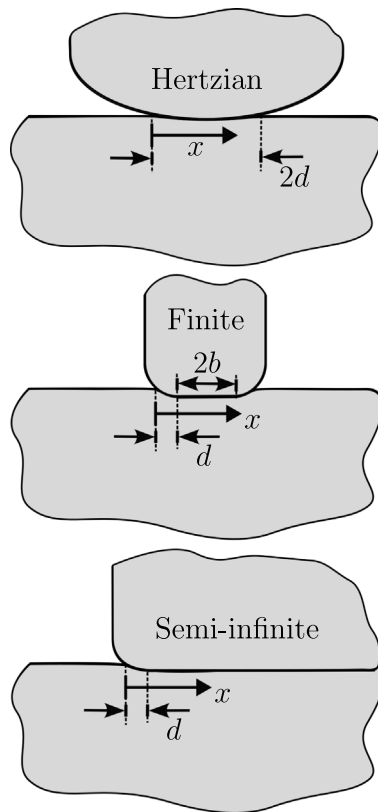
(a) Diagrams of Hertzian, finite, and semi-infinite contacts with a half-plane. d is the length of the curved section in the contact and x is measured from the left contact edge.
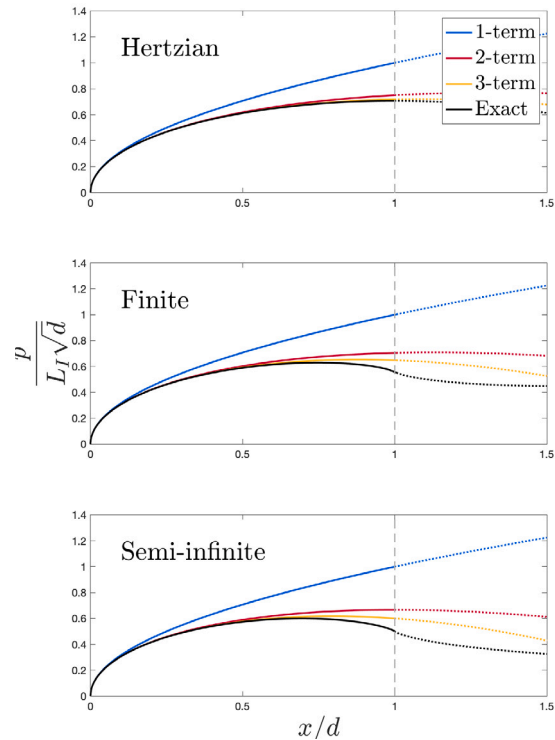
(b) The exact contact pressure for the three different contact cases (black), alongside one- (blue), two- (red), and three-term (orange) approximations. The dashed parts of the curves denote the flat part of the contact, while the solid curves represent the curved part of the contact.

Fig. 2. Contact pressure asymptotic expansion plots for three different types of contacts: Hertzian ($b/d \to 0$, top), finite ($b/d = 0.515$, middle) and semi-infinite ($b/d \to \infty$, bottom).

contact edge, where both domains can be appropriately represented by a half-plane.

As a means of analysing, in practical terms, how far the uncoupled solution deviates from the true coupled solution for the flat and rounded geometry, we will now derive the uncoupled solution from half-plane theory, for a semi-infinite flat punch with a rounded edge, pressed into an elastically similar half-plane. The uncoupled nature of the solution means that a normal load will induce a contact pressure alone, given in Eq. (9), which takes the asymptotic forms

$$p(x) = \frac{L_I d}{3\sqrt{x}} \equiv \frac{K_{I[1/2]}}{\sqrt{x}} \qquad x \gg d, \tag{14}$$

$$p(x) = L_I \sqrt{x} \qquad x \ll d, \tag{15}$$

and where the contact law is given by

$$\frac{\pi R L_I}{2E^*} = \sqrt{d}, \tag{16}$$

or

$$\frac{d}{R} = \frac{\pi^2}{4} \widetilde{L_I}^2 \tag{17}$$

where $\widetilde{L_I} = R L_I / E^*$.

In addition, the solution derived in the half-plane formulation has the desirable property of being closed-form with a number of useful attributes, such as a contact law, Eqs. (16), (17). For example, it is straightforward to show that the maximum contact pressure is given by

$$\frac{p_0}{E^*} \simeq \sqrt[3]{1.24 \frac{\pi^4}{144} \widetilde{L_I}^2}. \tag{18}$$

Moreover, due to the uncoupled nature of the solution, the above also applies for a shear load inducing an alone shear traction,

$$q(x) = \frac{L_{II}}{4\sqrt{d}} \left[2\sqrt{dx} + (x - d) \ln \left| \frac{1 - \sqrt{x/d}}{1 + \sqrt{x/d}} \right| \right] \qquad x > 0. \tag{19}$$

where equations replace $p(x)$ with $q(x)$, and L_I with L_{II}, respectively.

As expected, the asymptotic approximation given by Eq. (1) takes the correct form when close to the contact edge, $x \ll d$, where the contact problem is appropriately represented by half-plane theory. However, the difficulty in using this solution is when the observation point is remote from the edge. As we see from Eq. (14), the contact pressure is seen to decay in an inverse square-root fashion. If we consider the geometry in Fig. 1, where both bodies are elastically similar, far from the edge of the contact, the geometry looks like a wedge of angle $3\pi/2$ radianss, not two half-planes. Therefore, we would expect the actual contact pressure decay along the interface to correlate with that found in the classical Williams' solution [9], which is not inverse square-root bounded. Here, the half-plane solution breaks down, away from the contact edge. In summary, the pressure distribution displayed in this section is considered valid when the observation point is near the contact edge, i.e. we can be confident that Eq. (9) accurately represents the contact pressure between a pair of contacting elastically similar bodies for small values of x/d. However, the solution falls apart as the observation point moves away from the contact edge; the decay rate is not what we would expect from consideration of Fig. 1 if the interface has remotely adhered due to the introduction of coupling.

As a result, it is justified to compare the half-plane formulation with an alternative formulation that is bounded by Williams' solution far from the contact edge to analyse the extent to which they diverge.

3.2. Three-quarter plane formulation

To overcome the problem that arises far from the contact edge, we must define the domain shape of the rounded edge body more rigorously.

Referring to Fig. 1, looking from an observation point well away from the contact edge, the pair of bodies behave like a square-edged quarter plane pressing onto an elastically similar half-plane. To permit the domain to be thought of as a three-quarter plane, — a bonded half-plane and quarter plane, or a wedge of angle $3\pi/2$, we must make the following assumptions: the bodies are both elastic and made from the same material (elastically similar), and the coefficient of friction is sufficiently large for the interface to be stuck away from the contact edge [2,16]. The eigenvector to Williams' solution dictates the ratio of shear to direct traction; the contact will be stuck provided the coefficient of friction is at least as big as this ratio. The ratio for a wedge of angle $3\pi/2$ radians is 0.543, and it is assumed, in the analysis, that the coefficient of friction is at least as big as this.[2]

When these considerations apply, the solution far from the contact edge should, instead of displaying a square root decay, follow Williams' solution [9,10]; for example, for the pure mode 1 loading case – relative to the bisector line – we should find $p \sim x^{\lambda_I - 1}$, where $\lambda_I = 0.445$.

We constructed a finite element three-quarter plane model with a rounded corner for the indenter, following the assumptions outlined above, based on the approach in [8,17]. In the finite element model, we apply displacement boundary conditions from Williams' solution, for a wedge of angle $3\pi/2$ radians, far from the contact edge [13].

3.3. Pure mode I loading

As a first step in understanding how the two solutions compare, we excite pure mode I loading only, in the wedge sense. We denote the corresponding stress intensity factor by $K_{I[3/4]}$, seen in Fig. 1.

Looking near the contact edge, as we change the normal loading and shear loading in proportion, the contact edge moves slightly due to the growth in contact size, and a bounded shear traction results. Therefore, when $x/d \ll 1$, we see each traction is described well by the following square root bounded asymptotes

$$p(x) = L_I \sqrt{x}, \tag{20}$$

$$q(x) = L_{II} \sqrt{x}. \tag{21}$$

The calibrations for the asymptote coefficients L_I and L_{II} are given in [17] (see Eqs. (3) and (8) therein), viz.

$$L_I = \left(\frac{-0.93 K_{I[3/4]}}{E^* R^{1-\lambda_I}} \right)^{1/3} \frac{E^*}{\sqrt{R}}, \tag{22}$$

$$L_{II} = \left(\frac{-0.04 K_{I[3/4]}}{E^* R^{1-\lambda_I}} \right)^{1/3} \frac{E^*}{\sqrt{R}}, \tag{23}$$

where we have set $K_{II[3/4]} = 0$ as we are considering pure mode I loading, and the mode I eigenvalue, $\lambda_I = 0.5445$, for the case of a $3\pi/2$ radians wedge [8].

These curves plotted in Fig. 3, coloured blue (broken) for pressure and orange (broken) for shear, are the point of commonality between the rounded three-quarter plane solution and the half-plane solution. With the multipliers, L_I and L_{II}, fixed at the contact edge, the traction distributions may be plotted from the closed-form equation for a half-plane Eqs. (9), (19). These are the smooth solid lines coloured blue (contact pressure) and orange (shear traction).

Theoretically, the half-plane formulation should only be valid when $x/d \ll 1$. However, as may be seen over the interval of Fig. 3, $0 < x/d < 4$, these lines are almost coincident with those from the numerical three-quarter plane analysis. This gives us confidence that we now have, for practical purposes, solutions for the tractions at the contact edge in closed form; the only multipliers on the solution are numerically determined for pure mode I loading, L_I and L_{II}.

Now, looking away from the contact edge, we must first check the two formulations fall to their asymptotic forms, and then analyse the extent to which the two solutions diverge from each other along the interface.

If we multiply the stress intensity factor, $K_{I[3/4]}$, by its corresponding eigenvector, we can easily find the tractions appearing along the interface. When $x/d \gg 1$ these solutions will apply. Fig. 4 shows these asymptotes by a dotted purple line (contact pressure) and a dotted yellow line (shear traction). The actual traction distributions along the interface in the rounded three-quarter plane analysis, extracted from the finite element simulations, are coloured solid purple (contact pressure) and solid yellow line (shear traction). In the same figure, we show the tractions from the half-plane analysis as given by Eqs. (9), (19): solid blue line (contact pressure) and solid orange line (shear tractions), are also plotted together with their square-root decay forms: dotted blue line (contact pressure) and dotted orange line (shear tractions) in Fig. 4.

We can infer two important points from Fig. 4. Firstly, we may be reassured that the distributions go to the correct asymptotic forms when $x/d \gg 1$, i.e. the tractions for both the half-plane and the finite element formulation approach their corresponding asymptotic forms as $x/d \to \infty$. Secondly, and more importantly, it is clear that the asymptotes for the half-plane formulation are quite distinct from those implied by the three-quarter plane analysis, particularly in the case of the shear tractions. For example, at the arbitrary far distance of $x/d = 1500$ from the contact edge, the magnitude of the error of the half-plane formulation compared to the three-quarter plane (Williams') solution, is 8.23% and 40.8% for the normal and shear tractions, respectively. The large errors here again illustrate the limitations of relying solely on half-plane theory in our approximations.

3.4. Pure mode II loading

This section provides an equivalent commentary to that given previously for pure mode II loading. Here, we reworked the finite-element model used in [8] for pure mode II loading only, in the wedge sense. The corresponding stress intensity factor is denoted by $K_{II[3/4]}$, seen in Fig. 1.

To begin with, we will study the tractions resulting near the edge of the contact. As mentioned previously, proportional loading of the contact results in a bounded shear traction at the contact edge; when $x/d \ll 1$, the tractions are well described by the square root bounded asymptotes, Eqs. (20), (21). For pure mode II loading, $K_{I[3/4]} = 0$, the calibrations from [17] can be written in the form

$$L_I = \left(\frac{0.981 K_{II[3/4]}}{E^* R^{1-\lambda_{II}}} \right)^{1/3} \frac{E^*}{\sqrt{R}} \tag{24}$$

$$L_{II} = \left(\frac{0.04 K_{II[3/4]}}{E^* R^{1-\lambda_{II}}} \right)^{1/3} \frac{E^*}{\sqrt{R}}, \tag{25}$$

where $\lambda_{II} = 0.9082$ is the mode II eigenvalue for the case of a $3\pi/2$ radians wedge [8].

As for pure mode I loading, Eqs. (20), (21), are the point of commonality between the rounded three-quarter plane solution and the half-plane solution. Fig. 5 displays these near-edge asymptotes, coloured blue (broken) for pressure and orange (broken) for shear. With the multipliers fixed at the contact edge, the normal and equivalent shear tractions are plotted from the closed-form half-plane solution, Eqs. (9),
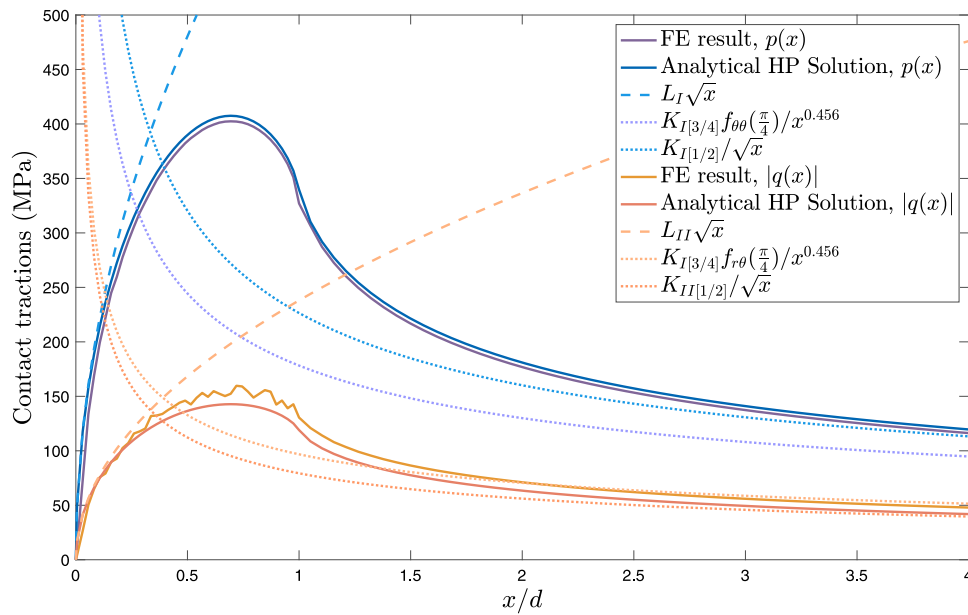
---

[2] At the outset, it is not clear that this condition will also maintain stick at the contact edge where the theory does not apply; but, in anticipation of results found later, we state that if the friction is sufficiently high to ensure stick in the interior it will also ensure stick at the edge under proportional loading conditions; other load paths are outside the scope of the current analysis.

Fig. 3. Pure mode 1 normal and shear tractions calculated using a three-quarter plane (FE result), and half-plane (analytical half-plane solution) formulations. These tractions are plotted alongside their near (broken line) and far (dotted line) asymptotes.
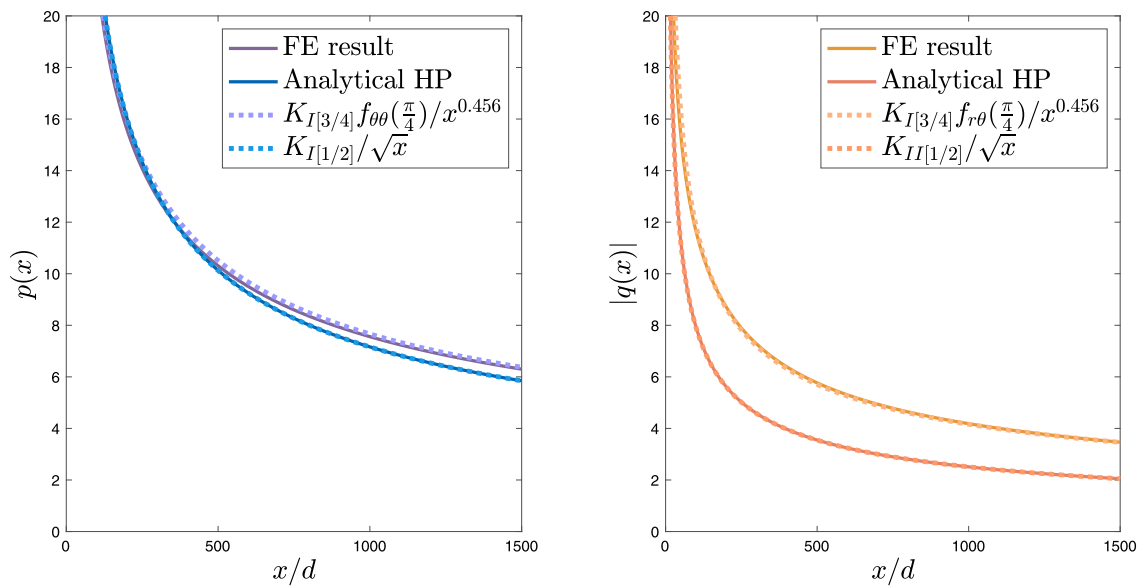

Fig. 4. Normal (left) and shear (right) tractions (solid lines) plotted against the half-plane and three-quarter plane decay asymptotes (dotted lines), far from the contact edge.

(19). These are shown in Fig. 5 by the smooth solid blue (contact pressure) and orange (shear traction) lines, alongside the tractions which emerge from the rounded three-quarter plane formulation, plotted in solid purple (contact pressure) and yellow (shear traction).

Theoretically, the half-plane formulation should only be valid when $x/d \ll 1$. However, as seen in Fig. 5, the half-plane solution is, again, almost coincident with the distributions obtained from the numerical three-quarter plane analysis for $0 < x/d < 4$. This is very encouraging, for practical purposes; it implies that we now have closed-form solutions for the tractions at the contact edge, with only the multipliers numerically determined, for both pure mode I and II loading.

As before, looking away from the contact edge (i.e. for $x/d \gg 1$), we must study two key areas: (1) that the two formulations fall to their corresponding asymptotic forms, and (2) the extent to which the two formulations diverge from each other. We address this in Fig. 6. For $x/d \gg 1$, the tractions along the interface for the half-plane formulation, are inverse square-root bounded, Eq. (14) and these are illustrated

by the blue dotted line (contact pressure) and the orange dotted line (shear traction). However, the tractions far from the contact edge, along the interface, can be correctly described by Williams' solution. In pure mode II loading, this asymptotic decay can be found by multiplying the stress intensity factor, $K_{II[3/4]}$, by its corresponding eigenvector. These decay asymptotes are plotted in Fig. 6 by a dotted purple line (contact pressure) and dotted yellow line (shear traction).

As encountered for pure mode I loading, we can use Fig. 6 to infer two key points. First of all, Fig. 6 provides clear evidence that, for each case, the exact solutions (solid lines) approach their expected asymptotic forms (dotted lines) when $x/d \gg 1$. Moreover, we can see that the tractions arising along the interface when using a half-plane formulation are significantly different to those implied by a three-quarter plane analysis. This difference is even starker than the previous example: in pure mode II loading, the difference is distinct for both normal and shear tractions; at the arbitrary far distance of
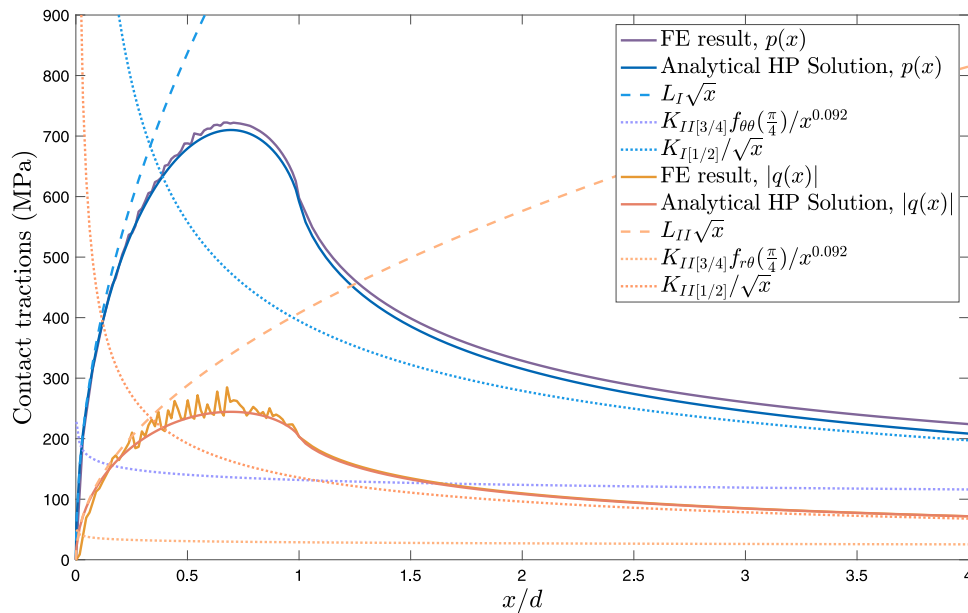
Fig. 5. Pure mode 2 normal and shear tractions calculated using a three-quarter plane (FE result), and half-plane (analytical half-plane solution) formulations. These tractions are plotted alongside their near (broken line) and far (dotted line) asymptotes.
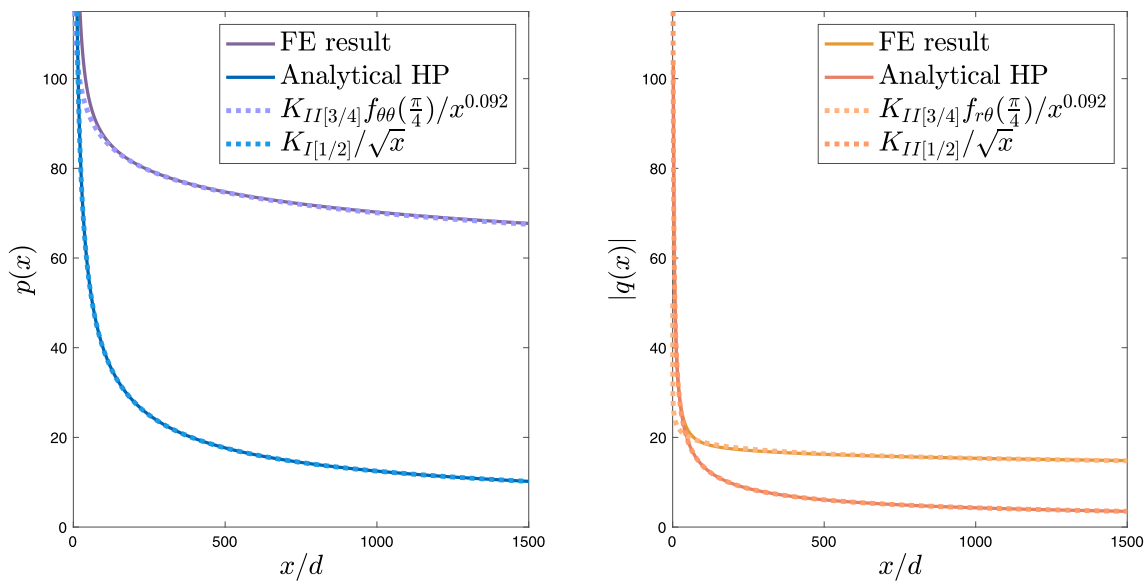

Fig. 6. Normal (left) and shear (right) tractions (solid lines) plotted against the half-plane and three-quarter plane decay asymptotes (dotted lines), far from the contact edge.

$x/d = 1500$ from the contact edge, the magnitude of the error of the half-plane formulation compared to the three-quarter plane solution is 84.8% and 76.1% for the normal and shear tractions, respectively. These results highlight the deficiency of relying, exclusively, on the half-plane formulation when observing the contact tractions far from the contact edge.

4. Conclusion

In this analysis, we have demonstrated the limitations of using an asymptotic representation of the state of stress for flat and rounded contacts. In such contacts, the regions of interest – typically slip zones – may extend a significant distance from the edge of the contact, well beyond the range of validity of such asymptotic approximations.

Aiming to solve this problem, we first turned to a half-plane for-mulation, aware that using the half-plane model in isolation may be poor due to the misleading representation of the contact-defining body. We noted that the decay of the state of stress implied by this solution, at remote points, was not of the correct form. This meant that we could not collocate the solution into any finite, slightly rounded contact problem.

We then looked at an FE solution to the geometrically exact slightly rounded three-quarter plane problem. We matched the very near-edge solution with that derived from half-plane theory, mentioned in the previous paragraph. The results from this analysis are very promising; the closed-form solution lies very close to the exact solution up to approximately $x/d = 5$ for both pure mode I and II loading. However, the poor assumptions implicit in the half-plane model become an issue when $x/d \gg 1$, as the model diverges from the exact solution in both loading case, as expected.

The formulation developed in this paper sets up the framework for a number of strands of investigation of the properties of slightly rounded

contacts — here limited to those in which the contact-defining body has a free surface normal to the contacting surface. We can now describe near-contact edge behaviour analytically, using Eqs. (9), (19), where the multipliers, L_I and L_{II} are rigorously, if numerically, related to the remote fields, Eqs. (22)–(25).

At the moment the remote fields have been chosen to be pure mode I and pure mode II only; the extension of the solution to other combinations or remote loading trajectories will form the next step. This extension has been foreshadowed in [18], but at that time, our understanding of the behaviour of incomplete frictional contact behaviour under varying normal loads was less well advanced. In particular, for such cases, we anticipate the closed-form half-plane solution will form an accurate asymptote for the mixed-mode finite element solution. This will permit us to find clean solutions for edge partial slip for this domain. Practical applications of these findings include fan blade dovetails in the root of a gas turbine and locking segments of riser-seabed connectors.

Declaration of competing interest

The authors declare that they have no known competing financial interests or personal relationships that could have appeared to influence the work reported in this paper.

Data availability

Data will be made available on request.

Acknowledgements

References

[1] Vingsbo O, Söderberg S. On fretting maps. Wear 1988;126(2):131–47.

[2] Churchman C, Mugadu A, Hills D. Asymptotic results for slipping complete frictional contacts. Eur J Mech A Solids 2003;22:793–800.

[3] Sackfield A, Mugadu A, Barber J, Hills D. The application of asymptotic solutions to characterizing the process zone in almost complete frictionless contacts. J Mech Phys Solids 2003;51:1333–46.

[4] Mugadu A, Hills D, Barber J, Sackfield A. The application of asymptotic solutions to characterizing the process zone in almost complete frictional contacts. Int J Solids Struct 2004;41:385–97.

[5] Montebello C, Pommier S, Karim D, Leroux J, Meriaux J. Analysis of the stress gradient effect in Fretting-Fatigue through nonlocal intensity factors. Int J Fatigue 2015;82.

[6] Ferry B, Araújo J, Pommier S, Karim D. Life of a Ti-6Al-4V alloy under fretting fatigue: Study of new nonlocal parameters. Tribol Int 2016;108.

[7] Cardoso R, Ferry B, Montebello C, Meriaux J, Pommier S, Araújo J. Study of size effects in fretting fatigue. Tribol Int 2019;143:106087.

[8] Fleury R, Hills D, Barber J. A corrective solution for finding the effects of edge-rounding on complete contact between elastically similar bodies. Part I: Contact law and normal contact considerations. Int J Solids Struct 2016;85.

[9] Williams M. Stress singularities resulting from various boundary conditions in angular corners of plates in extension. ASME J Appl Mech 1952;19(4):526–8.

[10] Barber JR. Elasticity. Solid mechanics and its applications, Springer Dordrecht; 2009.

[11] Moore M, Hills D. Analysing the accuracy of asymptotic approximations in incomplete contact problems. Int J Solids Struct 2022;253:111557.

[12] Andresen H, Hills D, Moore M. Representation of incomplete contact problems by half-planes. Eur J Mech A Solids 2021;85:104138, URL https://www.sciencedirect.com/science/article/pii/S099775382030526X.

[13] Hills D, Andresen H. Mechanics of fretting and fretting fatigue. 2021, p. 21–129. http://dx.doi.org/10.1007/978-3-030-70746-0.

[14] Mugadu A, Hills D, Barber J, Sackfield A. The application of asymptotic solutions to characterising the process zone in almost complete frictional contacts. Int J Solids Struct 2004;41:385–97.

[15] Sackfield A, Mugadu A, Barber J, Hills D. The application of asymptotic solutions to characterizing the process one in almost complete frictionless contacts. J Mech Phys Solids 2003;51:1333–46.

[16] Hills D, Thaitirarot A, Barber J, Dini D. Correlation of fretting fatigue experimental results using an asymptotic approach. Int J Fatigue 2012;43:62–75.

[17] Fleury R, Hills D, Barber J. A corrective solution for finding the effects of edge-rounding on complete contact between elastically similar bodies. Part II: Near-edge asymptotes and the effect of shear. Int J Solids Struct 2016;85.

[18] Fleury R. Investigation of fretting fatigue in turbine fir tree blade to disc joints at high temperature (DPhil thesis, University of Oxford) (Ph.D. thesis), 2015, p. 176.